

# Controlling quantum critical dynamics of isolated systems

A. del Campo<sup>1</sup> and K. Sengupta<sup>2</sup>

<sup>1</sup> Department of Physics, University of Massachusetts Boston, Boston, MA 02125, USA.

<sup>2</sup> Theoretical Physics Department, Indian Association for the Cultivation of Science, Jadavpur, Kolkata-700032, India.

**Abstract.** Controlling the non adiabatic dynamics of isolated quantum systems driven through a critical point is of interest in a variety of fields ranging from quantum simulation to finite-time thermodynamics. We briefly review the different methods for designing protocols which minimize excitation (defect) production in a closed quantum critical system driven out of equilibrium. We chart out the role of specific driving schemes for this procedure, point out their experimental relevance, and discuss their implementation in the context of ultracold atom and spin systems.

## 1 Introduction

The physics of closed quantum systems driven out of equilibrium has received a lot of theoretical and experimental attention in recent years. One of the central issues in this field involves understanding excitation or defect production resulting from a driving protocol. The associated dynamics becomes specially important when it involves the crossing of a quantum critical point [1,2,3,4,5]. The breakdown of adiabatic dynamics is often characterized by the probability of not ending up in the ground state which can be quantified using the density of excitations  $n$ . It is as well captured by the excess of energy over the instantaneous ground state  $E_0$ ,  $Q = \langle \psi | H | \psi \rangle - E_0$ . Many other quantities can be used, including the density of topological defects [6,7] (related to, but different from  $n$  [8,9]), the fidelity, etc. It is well known that when the crossing of a quantum critical point is induced by a slow linear quench of a parameter of the system Hamiltonian at a given rate  $\omega$ , a universal scaling law is observed. For instance, the excitation density  $n$  and the residual energy  $Q$  exhibit a power-law behavior

$$n \sim \omega^{d\nu/(z\nu+1)}, \quad Q \sim \omega^{(d+z)\nu/(z\nu+1)}, \quad (1)$$

where  $d$  is the dimension of the system and  $z$  and  $\nu$  are the dynamic and correlation length critical exponents [6,7,10,11,8,12]. Recent findings suggest that analogous signatures of universality are still present in dynamics of strongly-coupled systems, e.g., described by holographic duality [13,14,15]. Such scaling laws can also be extended to cases where the system passes through a critical surface [16], for non-linear ramps [17,18,21,19,20] and in the presence of an external control parameter with a self-consistent dynamics [22], and indicate an inevitable growth of  $n$  with increasing  $\omega$ . The root of such an increase owes its existence to the very nature of the critical point; as the characteristic energy gap  $\Delta$  closes in its neighbor-

hood, no drive can remain nearly adiabatic and the Landau criterion for excitation production  $d\Delta/dt \geq \Delta^2$  is always satisfied [10].

Such an increase of  $n$  and  $Q$  is, however, disadvantageous for the purpose of quantum computation, quantum state preparation, the control of non adiabatic processes in quantum critical system, and that of the associated work fluctuations, of interest to optimize the efficiency of quantum devices operating at the nanoscale. In all these cases, it is necessary to implement dynamical protocols which take a quantum system from one state to another in a finite amount of time. To this end, a quantum system is typically prepared in its ground state  $|\psi_0\rangle$  for given values of the control parameters  $\{\lambda_i\}$  of the system Hamiltonian  $H_0[\{\lambda_i\}]$ . Subsequently, a dynamics is induced by either changing these parameters as a function of time  $\{\lambda_i \equiv \lambda_i(t)\}$ , or by subjecting the system to an external possibly time-dependent perturbation  $H_1(t)$  for a pre-determined finite amount of time  $T$ . The resulting quantum evolution, governed by the time-dependent Schrödinger equation  $i\hbar\partial_t|\psi(t)\rangle = [H_0(t) + H_1(t)]|\psi(t)\rangle$ , takes the system to a new state  $|\psi_f\rangle \equiv |\psi(T)\rangle$  at the end of the process. The question arises as to how a specific final quantum state can be reached  $|n\rangle$  at the end of the evolution with close to unit fidelity, i.e., ensuring that  $|\langle n|\psi_f\rangle|^2 \simeq 1$ . If  $|n\rangle$  happens to be the ground state of the final Hamiltonian, a unit fidelity can be achieved via a reduction of the formation of excitations during the dynamics, or what appears to be more challenging, by canceling excitations in a non adiabatic protocol upon completion of the process. We shall see that a variety of shortcuts to adiabaticity in critical systems achieved the latter goal.

At this stage, let us clarify that we shall focus exclusively on driven systems which obey unitary dynamics and that are described by a time-dependent Hamiltonian. Hence, we consider systems decoupled from the surrounding environment, up to the set of external control parameters. Consequently, we shall not dwell on the possible use of the environment to reduce excitation formation [23,24], the design of open quantum dynamics [25], or the use of Hamiltonian quantum controls to effectively decouple the system from its environment [26,27,28]. We note that even within this restricted territory, efforts to guide the non adiabatic dynamics of driven quantum systems while mimicking adiabaticity have already led to a broad variety of theoretical and experimental results scattered in the literature [29,30,31,32,33,4,34], with applications to quantum fluids [35,36,37,38,39,40,41,42,43,44,45], trapped ions [46,47,48,49,50,51] and effective few-level systems [29,30,52,53,54,55]. In this review, we shall focus on an prominent sub-area, namely, the control of quantum critical dynamics [56,57,17,58,21,59,60,61,62,63]. The purpose of the present review is to briefly outline some recent developments aimed at tailoring, controlling and reducing excitation formation in driven quantum critical systems and discuss the feasibility of their implementation in realistic experimental systems.

A natural strategy to warrant an excitation-free evolution in finite-size gapped systems is to comply with the adiabatic theorem [64,65]. Excitation formation is suppressed whenever the quench time is longer than the inverse of a given power of the minimum energy gap, that can be efficiently computed, see e. g., [66].

Whenever the critical point is precisely known and an exquisite control of the external parameter is available, knowledge of the scaling laws in (1) can be used to design optimal nonlinear quenches for which the excitation density is reduced given a fixed duration of the process [17,63,2]. One can also resort on a more general, yet smooth time-dependence of the external control [67].

As an alternative, in spatially extended systems with finite range interactions one can implement an inhomogeneous driving. In such scenario, criticality is first reached locally in a finite region of the system, whose spatial extent grows subsequently with time. Tuning the velocity of the critical front paves the way to a fully adiabatic crossing of the phase transition whenever its value does not surpass the second sound velocity [56,57]. This idea was introduced in a classical setting [56,57,58,68,69,70] and has been experimentally explored in the context of kink formation in trapped ion chains [71,72,73,74] and soliton creation in harmonically confined Bose-Einstein condensates [75]. However, its key tenets have been shown to hold in quantum systems as well [76,77,78,79,80] (see Ref. [61] for an updated account).

In what follows, we shall focus on three techniques to mimic adiabaticity. The first of these is generally referred to as the counterdiabatic driving technique and was introduced by Demirplak and Rice [29], and elaborated by Berry [30] (see also Ref. [81]). It involves a modification of the system Hamiltonian  $H_0(t)$  by a suitably chosen auxiliary term  $H_1(t)$ . In this protocol,  $H_1(t)$  is chosen so that the adiabatic approximation to  $H_0(t)$  becomes the exact solution of the many-body time dependent Schrödinger equation with  $H(t) = H_0(t) + H_1(t)$  [29,30]. Such a procedure has been studied for several systems including a large variety of single-particle, many-body and nonlinear systems [29,30,60,44,51,42]. In quantum critical systems, its experimental implementation is expected to be complicated as the auxiliary term is generally nonlocal and include many-body interactions, although its form can be suitably tailored under given resources [34,82]. The second class of methods involve designing an optimal protocol that leads to maximal reduction of excitations for a fixed evolution time  $T$  [21,59,40]. Optimal protocols can be difficult to find for complicated interacting quantum systems; however, they have been computed for specific many-body models [59,40]. Finally, the third approach involves simultaneous variation of two parameters of a system Hamiltonian [62]. The first of these controls the proximity of the quantum system to the critical point while the second determines the phase space available for excitation production. This technique also applies to experimentally realizable non-integrable model [63]. While this method does not constitute an optimal protocol, its main advantage is the possibility relatively simple experimental implementation.

The rest of this article is organized as follows. We devote Sec. 2 to counterdiabatic driving, Sec. 3 to the applications of the optimal control in excitation suppression and Sec. 4 to the two-rate protocol. We close with a discussion in Sec. 5.

## 2 Counterdiabatic driving

In this section, we review the counterdiabatic driving technique also known as transitionless quantum driving [29,30]. The key idea behind this approach is to find an auxiliary counterdiabatic Hamiltonian  $H_1(t)$ , which when added to the system Hamiltonian  $H_0(t)$  ensures that the adiabatic approximation to  $H_0(t)$  becomes the exact solution to the dynamics generated by  $H(t) = H_0(t) + H_1(t)$ , even in the absence of slow driving. As a result,  $H(t)$  drives a “fast-motion video” of the adiabatic dynamics associated with  $H_0(t)$ . The form of  $H$  corresponding to a given  $H_0$  can be obtained as follows. Consider the Schrödinger equation

$$H_0(t)|n\rangle = E_n(t)|n\rangle, \quad (2)$$

where  $\{E_n(t)\}$  and  $\{|n(t)\rangle\}$  denote the set of instantaneous eigenvalues and eigenstates, respectively. Next, select as a target trajectory,

$$|\psi_n\rangle = e^{-\int_0^t dt' [iE_n(t')/\hbar + \langle n|\partial_{t'} n\rangle]} |n\rangle, \quad (3)$$

i.e., the adiabatic evolution of  $|n\rangle$  which would only describe the dynamics generated by  $H_0(t)$  under slow driving. Note that the phase factor in Eq. (3) incorporates the dynamic contribution as well as the geometric phase, generated by the Berry potential  $A_n(t') = i\langle n|\partial_{t'} n\rangle$ . One then needs to design a Hamiltonian  $H(t)$  which satisfies

$$i\hbar\partial_t|\psi_n\rangle = H(t)|\psi_n\rangle = [H_0(t) + H_1(t)]|\psi_n\rangle, \quad (4)$$

so that  $|\psi_n(t)\rangle$  remains the instantaneous ground state of  $H_0$  up to a phase. The spectral decomposition of the time-evolution operator simply reads  $U(t,0) = \sum_n |\psi_n(t)\rangle\langle n(0)|$ , from which the required Hamiltonian can be derived using the identity

$$H(t) = i\hbar(\partial_t U(t,0))U(t,0)^\dagger. \quad (5)$$

It follows that

$$H(t) = \sum_n E_n |n\rangle\langle n| + \sum_n [i\hbar |\partial_t n\rangle\langle n| - \hbar A_n(t) |n\rangle\langle n|], \quad (6)$$

where the first and second terms on the RHS can be recognized as the system Hamiltonian and the auxiliary term, respectively. The latter can be rewritten as

$$H_1(t) = i\hbar \sum_{m \neq n} \sum_n \frac{\langle m | \partial_t H_0(t) | n \rangle}{E_n - E_m} |m\rangle\langle n|, \quad (7)$$

where  $|m\rangle, |n\rangle$  are the instantaneous eigenstates of  $H_0$  and we have assumed that the system is non-degenerate. As expected  $H_1(t)$  vanishes in the truly adiabatic limit while its norm increases with the rate of change of the system Hamiltonian along [29,60]. We note that computing  $H_1$  requires full knowledge of the instantaneous spectral properties of the system, i.e., that of  $\{E_n(t)\}$  and  $\{|n(t)\rangle\}$ . For a moderate system size this information can be accessed via numerical methods, while for arbitrary system size its determination becomes a theoretical challenge beyond simple integrable models.

This requirement can be removed by introducing hybrid methods relying on a combination of counterdiabatic driving and optimal control [83]. Indeed, a practical advantage of counterdiabatic driving lies in its power to determine approximate expressions of  $H_1$  leading to a controlled reduction, instead of a complete suppression, of excitation production during critical dynamics [60,82,83]. To this end, one can further exploit the freedom associated with the choice of the phase of  $|\psi_n\rangle$ , which need not include the dynamic and geometric contributions. This is, given a unitary  $G(t)$ , the time evolution along the trajectory  $G(t)|\psi_n\rangle$  is generated by a unitarily equivalent Hamiltonian

$$H_G = GHG^\dagger - i\hbar G \partial_t G^\dagger, \quad (8)$$

whose physical properties are normally completely different from those of  $H$  [84]. One can allow for excitations to occur along the dynamics and impose boundary conditions at the beginning and end of the protocol so that  $G(t)$  reduces then to the identity. This approach has proven extremely useful in designing experimentally-realizable shortcuts to adiabaticity [30,85,44,51] as demonstrated in quantum optical systems [52,54] and low-dimensional quantum gases [45], while realizations in critical systems remain to be explored.

Before considering the dynamics across critical point, it is illuminating to understand the counterdiabatic driving of single-particle problems. A specific instance of such a problem which is of direct relevance to many-body systems is the time-dependent two-level system whose Hamiltonian is given by

$$H_0(t) = \lambda(t)\sigma_z + \Delta\sigma_x, \quad (9)$$

with instantaneous eigenenergies  $E_\pm(t) = \pm\sqrt{\lambda^2(t) + \Delta^2}$ . The avoided level crossing for such a system takes place at  $\lambda(t) = 0$ . Then, a straightforward calculation leads to [29]

$$H_1(t) = -\frac{\Delta \partial_t \lambda(t)}{2(\lambda^2(t) + \Delta^2)} \sigma_y. \quad (10)$$

This result can be directly applied to a class of integrable models known as quasi-free fermion systems that includes paradigmatic models in statistical mechanics such as the Ising and the XY models in  $d = 1$  and the Kitaev model in  $d = 2$  [60]. In what follows we are going to discuss the Ising model explicitly. The Hamiltonian of the Ising model for  $d = 1$  is given by

$$H_0 = -\sum_{\langle ij \rangle} S_i^z S_j^z + g(t) \sum_i S_i^x, \quad (11)$$

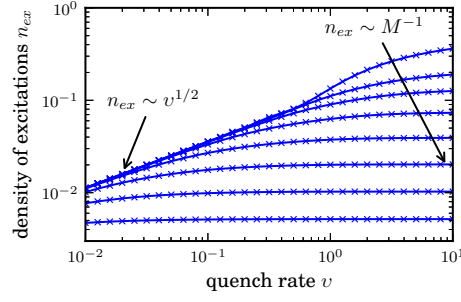


**Fig. 1.** (Color online) Reduction of excitation density in a 1D Ising chain quench through its critical point by a ramp of the transverse field. The exact auxiliary counterdiabatic driving term  $H_1$  involves multi-body interactions which extend over the whole system. A direct real-space truncation of  $H_1$  effectively suppresses excitations with wave vector  $k > 1/M$ , whenever  $H_1$  includes interactions of up to  $M$ -spins. The value of  $M$  is chosen to be 0, 1, 2, 4, 8, 16, 32 and 64 from top to bottom. The figure demonstrates a gradual suppression of excitation density as the cutoff  $M$  is increased. Taken from [60].

where  $g(t)$  denotes a time-dependent dimensionless transverse magnetic field,  $S_i^{x,z}$  denotes the spin operators on the  $i^{\text{th}}$  site of the 1D lattice, and  $\langle ij \rangle$  indicates that  $i$  and  $j$  are neighboring sites. Such a Hamiltonian can be mapped, via well-known Jordan-Wigner transformation, to a set of fermionic two-level systems whose Hamiltonian is given by  $H_0 = \sum_{k>0} \psi_k^\dagger H_k \psi_k$ , where  $\psi(k) = (c_k, c_{-k}^\dagger)$  are two component Fermion operators and  $H_k$  is given by

$$H_k = 2[g(t) - \cos(k)]\sigma_z + \sin(k)\sigma_x. \quad (12)$$

Using Eq. (10), one can thus write an expression for  $H_1(t)$  [60]

$$H_1 = - \sum_{k>0} \frac{\sin(k) \partial_t g(t)}{2[1 + g^2(t) - 2g(t) \cos(k)]} \psi_k^\dagger \sigma_y \psi_k. \quad (13)$$

The neat form of  $H_1$  in the Fermion language is not preserved in spin-space [60]. Indeed, a reverse Jordan-Wigner transformation reveals that  $H_1$  involves multiple spin terms. Explicitly, for an even number of spins under periodic boundary conditions  $H_1$  takes the form

$$H_1 = - \frac{dg}{dt} \sum_{m=1}^{N/2} h_m(g) H_1^{[m]}, \quad (14)$$

where  $\{h_m(g)\}$  are real coefficients decaying over the equilibrium correlation length and  $H_1^{[m]}$  involves  $m$ -body interaction extended over  $m$  adjoint spins. The efficiency of an approximate expression obtained by direct truncation in spin-space restricting the sum to  $M < N/2$  is shown in Fig. 1 and it clearly demonstrates a reduction of the excitation density as  $M$  is increased. Similarly, the general counterdiabatic driving term for quasi-free fermion systems was presented in ref. [60], and is generally expected to be nonlocal. The reader is referred to Ref. [86] for a detailed discussion of counterdiabatic driving in the XY model and the Lipkin-Meshkov-Glick model in the thermodynamic limit. However, for the typical number of spins of relevance to current efforts in quantum simulation, finite size corrections play a key role and need to be taken into account as pointed out in [87,83].

As an alternative to the direct real-space truncation of  $H_1$ , one can adopt a practical approach and look for an approximate auxiliary term  $\tilde{H}_1 = \sum_k \alpha_k L_k$  realizable in terms of

the set  $\{L_k\}$  of available controls. The optimal value of the coefficients  $\alpha_k$  can be determined by a variational principle of the form [34,82]

$$\min_{\{\alpha_k(t)\}} \| (H_1 - \tilde{H}_1) |\psi_n(t)\rangle \|^2. \quad (15)$$

Tailoring the counterdiabatic auxiliary interactions in this way, it was shown that few-body short-range interactions suffice to generate an effectively adiabatic dynamics.

We shall close this section pointing out that the experimental implementations of counterdiabatic driving scheme in many-body systems could be pursued using stroboscopic techniques [88] for digital quantum simulation with either trapped ions [89,90] or polar molecules [91].

### 3 Optimal Control Methods

The method of optimal control exploits variational calculus to determine a driving protocol which minimizes a given cost function, e.g., the density of excitations. A variety of methods have been proposed in the literature [92].

In the context of quantum critical dynamics, the determination of the optimal non-linear ramp driving a phase transition was discussed in Ref. [21]. Consider a modulation of a Hamiltonian parameter  $g$  described by  $g(t) = g_0 |t/T|^r$  during the interval  $[-T, T]$ , according to which the critical point is crossed at  $t = 0$ . It can be shown [21] that the optimal protocol for minimization of defect production occurs when the exponent  $r$  is chosen to be

$$r = -(z\nu)^{-1} \ln[\delta C^{-1} \ln(C/\delta)], \quad (16)$$

where  $C$  is a non-universal system-specific constant of the order unity,  $z$  and  $\nu$  are the dynamic and correlation length critical exponents,  $\delta = 1/(T\Delta_0)$ , and  $\Delta_0$  is a typical low-energy scale in the system for  $g = g_0$  [21]. This non-trivial optimal power for  $r$  is a function of the passage time but is independent of the dimension of the system. The defect density  $n_{\text{opt}}$  produced during such a drive scales as

$$n_{\text{opt}} \simeq [\delta C^{-1} \ln(C/\delta)]^{d/z} \quad (17)$$

and satisfies  $n_{\text{opt}} \ll n_{\text{lin}}$ , where  $n_{\text{lin}}$  is the defect density generated due to a linear ramp ( $r = 1$ ).

The above analysis relies on universal dynamics of phase transitions. A more systematic approach to suppress excitations is based on recasting the minimization problem as a standard problem in optimal control theory [92], a strategy explored in a recent series of works [93,59,40,94,95,96]. Assume a quantum system with a Hamiltonian of the form  $H_0 = \sum_{i=1,N} \lambda_i h_i$  where  $h_i$  are local operators with dimensions of energy and  $\lambda_i$  are the corresponding dimensionless couplings. Let the system be initialized in its ground state  $|\psi_1\rangle$  for  $\{\lambda_i\} = \{\lambda_0\}$  and consider a modulation of the system Hamiltonian such that  $\{\lambda_i(T)\} = \{\lambda_f\}$ , with  $|\psi_2\rangle$  being the ground state of  $H(\{\lambda_f\})$ . Denoting the state of the system at the end of the evolution is  $|\psi_T\rangle$ , one looks for an optimal time-dependence of  $\{\lambda\}$  which maximizes the overlap  $|\langle\psi_T|\psi_2\rangle|^2$ . As expected, the result turns out to be system specific and to date, solutions are known for a few model system only [59,40]. In particular, determining the optimal protocol in high dimensional ( $d > 1$ ) non-integrable interacting quantum many-body Hamiltonians constitutes an important open problem in the field.

To illustrate the method, we follow ref. [40], and choose the Luttinger liquid (LL) as the specific system at hand. The Hamiltonian of the LL in the bosonic representation reads

$$H_{\text{LL}} = u \sum_k [K \Pi_k \Pi_{-k} + K^{-1} k^2 \phi_k \phi_{-k}], \quad (18)$$



where  $u$  and  $K$  are the velocity of the charge carriers and the Luttinger parameter, respectively. Here,  $\phi_k$  denotes a bosonic field with momentum  $k$  and  $\Pi_k = -i\partial_{\phi_k}$  is the conjugate momentum operator. We note that  $H_{\text{LL}}$  is the low energy representation of the 1D Hubbard model on a lattice

$$H_{\text{Hubbard}} = \sum_i \left[ -(c_i^\dagger c_{i+1} + \text{h.c.}) + V \hat{n}_i \hat{n}_{i+1} \right], \quad (19)$$

where  $i$  denotes lattice coordinate,  $c_i$  is the annihilation operator for the bosons at site  $i$ , and  $\hat{n}_i = c_i^\dagger c_i$  is the fermion number operator. The LL description of the low-energy sector of this model holds for  $-2 < V < 2$  where the system is gapless; for  $|V| > 2$ , a charge-density wave (CDW) gap opens up. The parameter  $V$ , in the LL regime, can be related to  $K$  and  $u$  directly via Bethe Ansatz, see e.g., ref. [97].

Let us consider the system to be in its critical point at  $V = 2$  and study the dynamics induced by a change of  $V$ , or equivalently,  $u$  and  $K$ . We shall assume that this dynamics can be described in terms of LL Hamiltonian with  $u \equiv u(t)$  and  $K \equiv K(t)$ . Using  $\Pi_k = -i\partial_{\phi_k}$  and solving the Schrödinger equation for the many-body wavefunction  $|\psi\rangle = \prod_k |\psi_k\rangle$ , it follows that

$$\{i\partial_t - u(t)[-K(t)/4(\partial_k^2) + k^2\phi_k^2/K(t)]\}|\psi_k\rangle = 0, \quad (20)$$

which has a straightforward solution for  $\psi_k = \langle k|\psi_k\rangle$ :

$$\begin{aligned} \psi_k &= (2k\text{Re}[z_k(t)]/\pi)^{1/4} e^{-kz_k(t)\phi_k^2}, \\ i\partial_t z_k(t) &= ku(t)K(t)[z_k(t)^2 - 1/K^2(t)]. \end{aligned} \quad (21)$$

To find the optimal protocol, the total evolution time is divided into  $N$  grids of width  $\Delta t$  such that  $V(t)$  can be represented by constant potential  $V_j$  in the  $j^{\text{th}}$  interval. Since a constant  $V_j$  corresponds to a constant  $u \equiv u_j$  and  $K \equiv K_j$ , a recursive solution for  $z_k^j$  can be derived

$$z_k^j = iK_j^{-1} \tan[ku_j \Delta t + \arctan[-iK_j z_k^{j-1}]]. \quad (22)$$

Its solution together with the knowledge of the final ground state suffices to compute the wavefunction overlap [40]. This is the quantity that acts as a cost function and whose optimization is achieved by varying the set of parameters  $u_j$  and  $K_j$  using Monte Carlo techniques [40]. We note that finding the cost function implies the calculation of the wavefunction overlap of the system for an arbitrary set of parameters. Whereas this allows for the determination of the optimal protocol, such a computation poses a challenge when the system at hand is non-integrable and of moderate size. We also note that the optimal control of integrable systems is of interest in its own right, and has been suggested as a route to universal quantum computation [98].

Optimal driving protocols have also been applied to other models such as the two-level system and the 1D Heisenberg spin chain [59]. One important aspect of such studies constitutes the relation of optimal-protocol design to the so called “quantum speed limit”, associated with a fundamental bound to the minimum time required for transition between two quantum states to occur, as dictated by Schrödinger dynamics. Early results restricted to time-independent Hamiltonians [99,100,101,102,103,104,105] have recently been extended to arbitrary driven systems in a variety of forms [106,107,59,108,109,110,111,112], although the question as to whether these new bounds are tight and reachable remains unresolved. With that caveat, the quantum speed limit for isolated driven systems reads [112]

$$T_{\text{QSL}} \geq \max \left\{ \frac{\hbar}{E}, \frac{\hbar}{\Delta E} \right\} \sin^2 \mathcal{L}(\psi_0, \psi_T). \quad (23)$$

Here, the angle between the states  $\psi_0$  and  $\psi_T$  is measured by the Bures length,

$$\mathcal{L}(\psi_0, \psi_T) = \arccos |\langle \psi_0 | \psi_T \rangle|. \quad (24)$$

The first part of the bound, known as the Margolus-Levitin (ML) [103], limits the speed of evolution by the inverse of mean energy,

$$\overline{E} = \frac{1}{T} \int_0^T \{ \langle \psi_t | H(t) | \psi_t \rangle - E_0(t) \} dt.$$

The second part of the bound generalizes to driven systems the Mandelstam-Tamm (MT) time-energy uncertainty relation [99,100,101,106,102,105], where the time-averaged squared root of the energy variance reads

$$\overline{\Delta E} = \frac{1}{T} \int_0^T \sqrt{\langle \psi_t | H(t)^2 | \psi_t \rangle - \langle \psi_t | H(t) | \psi_t \rangle^2} dt.$$

Using a variant of this result [107], it was shown in Ref. [59] that if the evolution time  $T$  happens to be shorter than  $T_{\text{QSL}}$ , the optimization algorithms do not converge. The power of this conclusion arises from the fact that it is independent of the protocol chosen for the drive; hence it provides a completely general bound for the maximum speed attainable via optimal control. Quantum speed limits also determine the solution of the quantum brachistochrone problem aimed at the preparation of a target state in a minimum time starting from a given initial state [113,114,55,115].

## 4 Two-rate dynamics

In this section, we review the details of a third method, namely, the suppression of defect density on passage through a quantum critical point when two parameters of the Hamiltonian are simultaneously varied in time [62,63]. The method relies on reducing the available phase space for excitation production using a second control parameter. Such a reduction does not necessarily lead to perfect shortcut to adiabaticity; however, the method has the advantage of relatively straightforward experimental implementation.

To provide a simple demonstration of this method, we first consider its application to integrable models such as the XY and the Kitaev models [62]. As discussed in Sec. 2, these models can be described in terms of non-interacting fermions via a Jordan Wigner transformation [60,16]. The Hamiltonian of such non-interacting fermions in  $d$ -dimensions can be written as  $H = \sum_{\mathbf{k}} \psi_{\mathbf{k}}^\dagger H_{\mathbf{k}} \psi_{\mathbf{k}}$  where  $\psi_{\mathbf{k}}^\dagger = (c_{1\mathbf{k}}^\dagger, c_{2\mathbf{k}}^\dagger)$  are Fermionic creation operators and  $H_{\mathbf{k}}(t)$  is given by

$$H_{\mathbf{k}}(t) = \tau_3(\lambda_1(t) - b_{\mathbf{k}}) + \tau_1 \lambda_2(t) g_{\mathbf{k}}. \quad (25)$$

Here  $\tau_3$  and  $\tau_1$  denote the usual Pauli matrices while  $b_{\mathbf{k}}$  and  $g_{\mathbf{k}}$  are general functions of momenta, and  $\lambda_{1(2)}(t) = \lambda_0 \omega_{1(2)} t$  are time dependent parameters driven with ramp rates  $\omega_{1(2)}$ . Note that in contrast to the usual driving schemes leading to the scaling laws in Eq. (1) where only  $\lambda_1$  is taken to be a function of time [1], we have chosen to vary the off-diagonal term  $\lambda_2$  as well. The instantaneous eigenvalues of the Hamiltonian is given by  $E_{\mathbf{k}}(t) = \pm \sqrt{(\lambda_1(t) - b_{\mathbf{k}})^2 + (\lambda_2(t) g_{\mathbf{k}})^2}$ . We assume that as a result of the ramps, the system reaches the critical point at  $t = t_{0\mathbf{k}_0} = b_{\mathbf{k}_0}/\omega_1$  and  $\mathbf{k} = \mathbf{k}_0$  where  $g_{\mathbf{k}_0} = 0$ .

It turns out that the Schrödinger equation corresponding to  $H_1(t)$  can be exactly solved. The key observation in this regard is that  $H_1$  can be written in terms of a set of new Pauli matrices  $\tilde{\tau}_3$  and  $\tilde{\tau}_1$  as follows,

$$H_{\mathbf{k}}(t) = \lambda_{1\mathbf{k}}(t - t_{1\mathbf{k}}) \tilde{\tau}_3 + \lambda_{2\mathbf{k}} \tilde{\tau}_1, \quad (26)$$



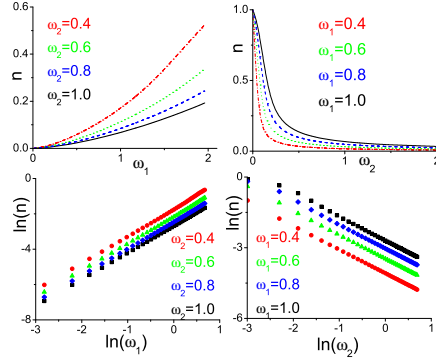


**Fig. 2.** (Color online) Top Panel: Plot of  $n$  vs  $\omega_1$  (left) and  $\omega_2$  (right) showing scaling of  $n$ . Bottom Panel: Plot of  $\ln(n)$  as a function of  $\ln(\omega_1)$  (left) and  $\ln(\omega_2)$  (right). All plots are computed using Eq. (28) with  $d = 1$ ,  $b_{\mathbf{k}} = 5 - \cos(k)$ , and  $g(k) = \sin(k)$  so that  $H$  represents 1D XY model in a transverse field. The scaling regime, where Eq. (29) holds, occur for  $\omega_2 \geq \omega_1^{3/2}/b_{\mathbf{k}_0} = 0.25\omega_1^{3/2}$ . Taken from [62].

where  $t_{1\mathbf{k}} = b_{\mathbf{k}}\omega_1/\lambda_{1\mathbf{k}}$ . In the above expression, the matrices  $\tilde{\tau}_{1,3}$  can be expressed in terms of  $\tau_{1,3}$  as

$$\begin{aligned}\lambda_{1\mathbf{k}}\tilde{\tau}_3 &= \omega_1\tau_3 + \omega_2g_{\mathbf{k}}\tau_1, \\ \lambda_{2\mathbf{k}}\tilde{\tau}_1 &= (\omega_1t_{1\mathbf{k}} - b_{\mathbf{k}})\tau_3 + \omega_2t_{1\mathbf{k}}g_{\mathbf{k}}\tau_1.\end{aligned}\quad (27)$$

Further, the quantities  $\lambda_{1\mathbf{k}}$  and  $\lambda_{2\mathbf{k}}$  are obtained by diagonalizing Eq. (27) [62]:  $\lambda_{1\mathbf{k}} = [\omega_1^2 + \omega_2^2g_{\mathbf{k}}^2]^{1/2}$  and  $\lambda_{2\mathbf{k}} = t_{1\mathbf{k}}[(\omega_2 - b_{\mathbf{k}}/t_{1\mathbf{k}})^2 + \omega_2^2g_{\mathbf{k}}^2]^{1/2}$ .

The above transformation shifts the entire time dependence of  $H_{\mathbf{k}}(t)$  to diagonal terms and reduces the corresponding Schrödinger equation to a set Landau-Zener problem (one for each mode  $\mathbf{k}$ ) [116]. Using the results of Refs. [116,117], one can thus simply read off the probability of excitation (defect) production for any  $\mathbf{k}$  to be  $p_{\mathbf{k}} = \exp[-\pi\lambda_{2\mathbf{k}}^2/\lambda_{1\mathbf{k}}]$  which leads to the defect density

$$n = \int d^d k / (2\pi)^d e^{-\pi\omega_2^2 b_{\mathbf{k}}^2 g_{\mathbf{k}}^2 / (\omega_1^2 + \omega_2^2 g_{\mathbf{k}}^2)^{3/2}}. \quad (28)$$

For  $\omega_{1,2}/b_{\mathbf{k}_0}^2 \ll 1$  and  $\omega_2/\omega_1 \geq \sqrt{\omega_1}/b_{\mathbf{k}_0}$ ,  $p_{\mathbf{k}}$  is appreciable around  $\mathbf{k} = \mathbf{k}_0$ . Thus in this regime, one can replace  $p_{\mathbf{k}}$  by its value around  $\mathbf{k}_0$  leading  $p_{\mathbf{k}} = e^{-c\omega_2^2 k^2/\omega_1^3}$ , with  $c = \pi b_{\mathbf{k}_0}^2$ . A simple rescaling of  $p_{\mathbf{k}}$ ,  $k' = k\omega_2/\omega_1^{3/2}$ , in this regime then leads to Eq. (28),

$$n \sim \omega_1^{3d/2} \omega_2^{-d}, \quad (29)$$

which demonstrates the suppression of the density of excitations with increasing  $\omega_2$ . Note that the validity of the scaling relations does not constrain  $\omega_2/\omega_1$  to small values; thus one can efficiently suppress defects by tuning  $\omega_2$  for a suitably chosen  $\omega_1$ . A plot of  $n$  computed from Eq. (28) with  $d = 1$ ,  $b_{\mathbf{k}} = 5 - \cos(k)$ , and  $g_{\mathbf{k}} = \sin(k)$  (chosen so that the model conforms to 1D XY model in a transverse field) is shown in top panels of Fig. 1 as a function of the rates  $\omega_1$  and  $\omega_2$ . The plot clearly demonstrates that  $n$  is a decreasing function of  $\omega_2$ .

Eq. (29) indicates the existence of two separate regimes  $n$  behaves qualitatively differently with  $\omega_1$  with  $\omega_2 = \omega_1^r$ . In one regime, where  $r \geq 3/2$ ,  $n$  increases  $\omega_1$  while it decreases

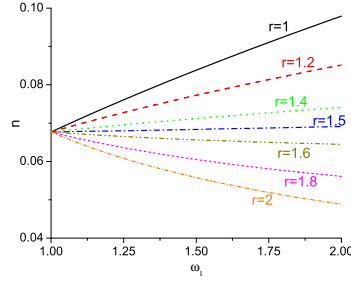


**Fig. 3.** Tailoring excitation formation by two-rate dynamics. Dependence of  $n$  on  $\omega_1$  with  $\omega_2 = \omega_1^r$  showing the crossover between regimes with increasing and decreasing  $n$  as a function of  $\omega_1$ . All parameters are the same as in Fig. 2. Taken from [62].

with  $\omega_1$  if  $r < 3/2$ . The crossover between these regimes occurs for  $\omega_2 = \omega_1^{r^*}$  with  $r^* = 3/2$  for any  $d$ . This crossover is indicated in Fig. 2, where  $n$  is plotted as function of  $\omega_1$  with  $\omega_2 = \omega_1^r$ . We note here that at  $r = r^*$ ,  $n$  becomes independent of  $\omega_1$  and  $\omega_2$ .

It turns out that it is relatively straightforward to generalize these concepts for arbitrary time dependent Hamiltonians. To see this, let us consider a generic Hamiltonian with two tunable parameters which are varied with rates  $\omega_1$  and  $\omega_2$ . The first parameter  $\lambda(t)$  controls its distance from a quantum critical point at  $\lambda = \lambda_c \neq 0$ ; this necessitates that the instantaneous energy gap near the critical point varies as  $\Delta(\mathbf{k} = \mathbf{k}_0; \lambda) \simeq |\lambda(t)|^{z\nu} = |\omega_1 t - \lambda_c|^{z\nu\alpha}$ , where  $\alpha$  is a positive exponent and  $\alpha = 1$  denotes linear drive protocol. The second parameter,  $c(t)$ , controls the dispersion of the quasiparticles at the critical point so that  $\Delta(k, \lambda_c) \simeq c(t)k^z = |\omega_2 t|^\beta k^z$ .

To estimate the defect density generated during such a drive, we first estimate the time spent by the system in the impulse region where defect production occurs (for small  $\omega_1$  it is also the critical region). For this, we use the well-known Landau criterion which states that a quantum system subjected to a drive is in the impulse region if  $d\Delta/dt \simeq \Delta^2$  [116,1]. Substituting the expression for  $\Delta(\mathbf{k}_0, \lambda(t))$  in this relation, one obtains an expression for  $T$ , the time spent by the system in the impulse region, as

$$|T - T_0| \simeq \omega_1^{-\alpha z \nu / (\alpha z \nu + 1)}, \quad (30)$$

where  $T_0 = \lambda_c/\omega_1$  is the time at which the system reaches the critical point. Substituting the expression for  $T$  in that for  $\Delta(\mathbf{k}_0, \lambda)$ , one finds that in the impulse region, the instantaneous energy gap behaves as

$$\Delta(\mathbf{k}_0; \lambda) \simeq \omega_1^{\alpha z \nu / (\alpha z \nu + 1)}. \quad (31)$$

Next, one notes that the defects or excitations are typically produced in a phase space  $\Omega \sim k^d$  around the critical mode. During the time  $T$  that the system spends in the impulse region, these momentum modes satisfy [118]

$$k \simeq |\omega_2 T_0|^{-\beta/z} \Delta(\mathbf{k}_0, \lambda(T))^{1/z} \quad (32)$$

Using Eqs. (30), (32) and (31), one finally gets

$$n \sim \Omega \sim k^d \simeq \omega_2^{-\beta d/z} \omega_1^{\left(\frac{\alpha \nu}{\alpha z \nu + 1} + \frac{\beta}{z}\right)d}. \quad (33)$$

which generalizes Eq. (29). The present analysis shows that the suppression of  $n$  with increasing  $\omega_2$  occurs due to the reduction of available momentum modes for quasiparticle

excitations at any given energy  $\Delta(k; \lambda)$ ; thus the role of the drive protocol changing  $c(t)$  is to reduce the available phase space for defect production. Analyzing Eq. (33), one finds  $r^* = 1 + \alpha z \nu / (\beta(\alpha z \nu + 1))$  which reduces to the condition  $r^* = 3/2$  derived earlier for  $\alpha = \beta = z = \nu = 1$ . We note in passing that Eq. (33) also constitute a generalization of Kibble-Zurek scaling laws for two-rate protocols.

As discussed in Ref. [62], there are several concrete models where the present method may be applied. However, it is perhaps more interesting to note that quantum systems near a phase transitions can often be described by a Landau-Ginzburg action which has the generic form

$$S = \int d^d r dt \psi^* [-\partial_t^2 + c_1 \sum_{i=1,d} \partial_{x_i}^2 + (r - r_c) - u|\psi|^2] \psi,$$

where  $r$  controls the distance to criticality while  $c_1$  controls the quasiparticle dispersion at criticality. Thus, if  $r$  and  $c_1$  are tuned as functions of time with rates  $\omega_1$  and  $\omega_2$ , one expects phase-space suppression leading to defect reduction as a function of  $\omega_2$ . This indicates that the suppression discussed above is of general nature. However, it is to be observed that  $r$  and  $c_1$  needs to be obtained from the microscopic parameters of the system action; thus whereas defect reduction occurs generically if  $c$  is increased, one still needs to specify the relation between the effective parameter  $c$  to microscopic parameters of  $H$  which can be experimentally tuned. This could be difficult for generic actions and specially so, for strongly interacting systems. Some progress in this direction has recently been made [63,120,121,119].

## 5 Conclusion

In this review, we have discussed several methods for tuning the excitation production in a closed quantum system during its passage through a quantum critical point. Among a broad variety of alternative routes to achieve this reduction, we have presented three techniques in detail. The first one, discussed in Sec.2, involves engineering an additional term  $H_1$  for the system Hamiltonian  $H_0$ , such that the dynamics generated by  $H(t) = H_0(t) + H_1(t)$  follows the adiabatic manifold of  $H_0$ . Determining the auxiliary term requires access to the spectral properties of the system  $H_0$  and its implementation might involve non-local multiple-body interactions. The strength of this method lies in the possibility of reducing excitation formation via approximate construction of  $H_1$  under given resources. The second method involves the determination of an optimal time-dependence of the system Hamiltonian  $H_0(t)$  using optimal control to maximize the overlap between the time evolving state and the target state, as discussed in Sec. 3. This method is mathematically rigorous; however, its implementation requires knowledge of the time-dependent many-body state of the system during the evolution which limits its applicability to moderate system sizes in non-integrable models. Finally, the two-rate protocol discussed in Sec. 4 exploits a two-parameter tuning of the system Hamiltonian. One of these parameters reduces the phase space available for excitation formation, and consequently, it suppresses defect production. While the method is not optimal, it allows in principle for an easy implementation in many-systems since only one additional parameter of the system Hamiltonian is to be tuned. However, the identification of the second drive parameter is system specific and at present, it has been theoretically tested for only a handful of non-integrable many-body systems.

It is our hope that the ideas summarized in this review contribute to deepen our understanding of the far-from-equilibrium dynamics of isolated quantum systems and related research areas. New theoretical and experimental developments can be expected pursuing applications of controlled quantum critical dynamics in the field of quantum simulation [122], thermalization of isolated quantum systems [5] and work fluctuations in finite-time thermodynamics [123]. The implications of these techniques in the design of new protocols to assist

and speed up quantum methods for optimization [124] constitute another research direction worth exploring.

We acknowledge B. Damski, S. Deffner, A. Dutta, S. Montangero, B. Peropadre, H. Saberi, J. D. Sau, D. Sen, and F. Setiawan for useful discussions and suggestions. AdC further thanks N. Guler for hospitality during the completion of the manuscript.

## References

1. A. Polkovnikov, K. Sengupta, A. Silva, and M. Vengalattore, *Rev. Mod. Phys.* **83**, 863 (2011).
2. J. Dziarmaga, *Adv. Phys.* **59**, 1063 (2010).
3. A. Dutta, U. Divakaran, D. Sen, B. K. Chakrabarti, T. F. Rosenbaum, and G. Aeppli, arXiv:1012.0653 (2010).
4. A. del Campo, W. H. Zurek, *Int. J. Mod. Phys. A* **29**, 1430018 (2014).
5. J. Eisert, M. Friesdorf, C. Gogolin, arXiv:1408.5148 (2014).
6. T. W. B. Kibble, *J. Phys. A: Math. Gen.* **9**, 1387 (1976); *Phys. Rep.* **67**, 183 (1980).
7. W. H. Zurek, *Nature (London)* **317**, 505 (1985); *Acta Phys. Pol. B* **24**, 1301 (1993); *Phys. Rep.* **276**, 177 (1996).
8. J. Dziarmaga, *Phys. Rev. Lett.* **95**, 245701 (2005).
9. M. Uhlmann, R. Schützhold, U. R. Fischer, *Phys. Rev. D* **81**, 025017 (2010).
10. B. Damski, *Phys. Rev. Lett.* **95**, 035701 (2005).
11. W. H. Zurek, U. Dorner, P. Zoller, *Phys. Rev. Lett.* **95**, 105701 (2005).
12. A. Polkovnikov, *Phys. Rev. B* **72**, 161201(R) (2005).
13. J. Sonner, A. del Campo, W. H. Zurek, arXiv:1406.2329 (2014).
14. P. M. Chesler, A. M. García-García, H. Liu, arXiv:1407.1862 (2014).
15. P. Basu and S. R. Das, *JHEP* **103**, 1201 (2012); P. Basu, D. Das, S. R. Das, and K. Sengupta, *JHEP* **12**, 1 (2013).
16. K. Sengupta, D. Sen and S. Mondal, *Phys. Rev. Lett.* **100**, 077204 (2008).
17. R. Barankov and A. Polkovnikov, *Phys. Rev. Lett.* **101**, 076801 (2008).
18. D. Sen, K. Sengupta and S. Mondal, *Phys. Rev. Lett.* **101**, 016806 (2008).
19. C. De Grandi, V. Gritsev, A. Polkovnikov, *Phys. Rev. B* **81**, 012303 (2010).
20. A. Chandran, A. Erez, S. S. Gubser, and S. L. Sondhi, *Phys. Rev. B* **86**, 064304 (2012).
21. A. Polkovnikov, *Phys. Rev. Lett.* **101**, 220402 (2008).
22. M. Kolodrubetz, E. Katz, A. Polkovnikov, arXiv:1406.2701 (2014).
23. D. Patanè, A. Silva, L. Amico, R. Fazio, G. E. Santoro, *Phys. Rev. Lett.* **101**, 175701 (2008).
24. D. Patanè, A. Silva, L. Amico, R. Fazio, G. E. Santoro, *Phys. Rev. B* **80**, 024302 (2009).
25. G. Vacanti, R. Fazio, S. Montangero, G. M. Palma, M. Paternostro, V. Vedral, *New J. Phys.* **16**, 053017 (2014).
26. L. Viola, S. Lloyd, *Phys. Rev. A* **58**, 2733 (1998).
27. L. Viola, E. Knill, S. Lloyd, *Phys. Rev. Lett.* **82**, 2417 (1999).
28. S. Sauer, C. Gneiting, and A. Buchleitner, *Phys. Rev. Lett.* **111**, 030405 (2013).
29. M. Demirplak and S. A. Rice, *J. Phys. Chem. A* **107**, 9937 (2003); *J. Phys. Chem. B* **109**, 6838 (2005); *J. Chem. Phys.* **129**, 154111 (2008).
30. M. V. Berry, *J. Phys. A: Math. Theor.* **42**, 365303 (2009).
31. X. Chen, A. Ruschhaupt, S. Schmidt, A. del Campo, D. Guéry-Odelin, J. G. Muga *Phys. Rev. Lett.* **104**, 063002 (2010).
32. E. Torrontegui, S. S. Ibáñez, S. Martínez-Garaot, M. Modugno, A. del Campo, D. Guéry-Odelin, A. Ruschhaupt, X. Chen, and J. G. Muga, *Adv. At. Mol. Opt. Phys.* **62**, 117 (2013).
33. C. Jarzynski, *Phys. Rev. A* **88**, 040101 (2013).
34. T. Opatrny, K. Mølmer, *New J. Phys.* **16**, 015025 (2014).
35. J. G. Muga, Xi Chen, A. Ruschhaupt, D. Guéry-Odelin, *J. Phys. B* **42**, 241001 (2009).
36. J.-F. Schaff, X.-L. Song, P. Vignolo, G. Labeyrie, *Phys. Rev. A* **82**, 033430 (2010).
37. J.-F. Schaff, X.-L. Song, P. Capuzzi, P. Vignolo, G. Labeyrie, *EPL* **93**, 23001 (2011).
38. D. Stefanatos, J. Ruths, J.-S. Li, *Phys. Rev. A* **82**, 063422 (2010).
39. A. del Campo, *Phys. Rev. A* **84**, 031606(R) (2011).

40. A. Rahmani and C. Chamon, Phys. Rev. Lett. **107**, 016402 (2011).
41. A. del Campo, M. G. Boshier, Sci. Rep. **2**, 648 (2012).
42. B. Julia-Díaz, E. Torrontegui, J. Martorell, J. G. Muga, and A. Polls, Phys. Rev. A **86**, 063623 (2012).
43. S. Choi, R. Onofrio, and B. Sundaram, Phys. Rev. A **84**, 051601(R) (2011).
44. A. del Campo, Phys. Rev. Lett. **111**, 100502 (2013).
45. W. Rohringer, D. Fischer, F. Steiner, I. E. Mazets, J. Schmiedmayer, M. Trupke, arXiv:1312.5948.
46. E. Torrontegui, S. Ibáñez, X. Chen, A. Ruschhaupt, D. Guéry-Odelin, J. G. Muga, Phys. Rev. A **83**, 013415 (2011).
47. R. Bowler, J. Gaebler, Y. Lin, T. R. Tan, D. Hanneke, J. D. Jost, J. P. Home, D. Leibfried, D. J. Wineland, Phys. Rev. Lett. **109**, 080502 (2012).
48. A. Walther, F. Ziesel, T. Ruster, S. T. Dawkins, K. Ott, M. Hettrich, K. Singer, F. Schmidt-Kaler, and U. Poschinger, Phys. Rev. Lett. **109**, 080501 (2012).
49. S. Masuda, Phys. Rev. A **86**, 063624 (2012).
50. M. Palmero, E. Torrontegui, D. Guéry-Odelin, and J. G. Muga, Phys. Rev. A **88**, 053423 (2013).
51. S. Deffner, C. Jarzynski, and A. del Campo, Phys. Rev. X **4**, 021013 (2014).
52. M. G. Bason, M. Viteau, N. Malossi, P. Huillery, E. Arimondo, D. Ciampini, R. Fazio, V. Giovannetti, R. Mannella, O. Morsch, Nature Phys. **8**, 147 (2011).
53. X. Chen, I. Lizuain, A. Ruschhaupt, D. Guéry-Odelin, J. G. Muga, Phys. Rev. Lett. **105**, 123003 (2010).
54. J. Zhang, J. Hyun Shim, I. Niemeyer, T. Taniguchi, T. Teraji, H. Abe, S. Onoda, T. Yamamoto, T. Ohshima, J. Isoya, D. Suter, Phys. Rev. Lett. **110**, 240501 (2013).
55. G. H. Hegerfeldt, Phys. Rev. Lett. **111**, 260501 (2013).
56. T. W. B. Kibble and G. E. Volovik, JETP Lett. **65**, 102 (1997).
57. J. Dziarmaga, P. Laguna, W. H. Zurek, Phys. Rev. Lett. **82**, 4749 (1999).
58. W. H. Zurek, Phys. Rev. Lett. **102**, 105702 (2009).
59. T. Caneva, M. Murphy, T. Calarco, R. Fazio, S. Montangero, V. Giovannetti, and G. E. Santoro, Phys. Rev. Lett. **103** 240501 (2009); T. Caneva, T. Calarco, R. Fazio, G. E. Santoro, S. Montangero, Phys. Rev. A **84**, 012312 (2011).
60. A. del Campo, M. M. Rams, and W. H. Zurek, Phys. Rev. Lett. **109**, 115703 (2012).
61. A. del Campo, T. W. B. Kibble, W. H. Zurek, J. Phys.: Condens. Matter **25**, 404210 (2013).
62. J. D. Sau, and K. Sengupta, Phys. Rev. B **90**, 104306 (2014).
63. U. Divakaran and K. Sengupta, arXiv:1408.4463 (2014).
64. S. Jansen, M.-B. Ruskai, and R. Seiler, J. Math. Phys. **48**, 102111 (2007).
65. V. Murg, J. I. Cirac, Phys. Rev. A **69**, 042320 (2004).
66. S. Mandrà, G. G. Guerreschi, and A. Aspuru-Guzik, arXiv:1407.8183 (2014).
67. D. A. Lidar, A. T. Rezakhani, and A. Hamma, J. Math. Phys. **50**, 102106 (2009).
68. A. del Campo, A. G. De Chiara, G. Morigi, M. B. Plenio, and A. Retzker, Phys. Rev. Lett. **105**, 075701 (2010).
69. A. del Campo, A. Retzker, and M. B. Plenio, New J. Phys. **13**, 083022 (2011).
70. E. Witkowska, P. Deuar, M. Gajda, and K. Rzażewski, Phys. Rev. Lett. **106**, 135301 (2011).
71. M. Mielenz, H. Landa, J. Brox, S. Kahra, G. Leschhorn, M. Albert, B. Reznik, T. Schaetz, Phys. Rev. Lett. **110**, 133004 (2013).
72. S. Ejtemaee and P. C. Haljan, Phys. Rev. A **87**, 051401(R) (2013).
73. S. Ulm, S. J. Roßnagel, G. Jacob, C. Degünther, S. T. Dawkins, U. G. Poschinger, R. Nigmatullin, A. Retzker, M. B. Plenio, F. Schmidt-Kaler, K. Singer, Nat. Commun. **4**, 2290 (2013).
74. K. Pyka, J. Keller, H. L. Partner, R. Nigmatullin, T. Burgermeister, D. M. Meier, K. Kuhlmann, A. Retzker, M. B. Plenio, W. H. Zurek, A. del Campo, and T. E. Mehlstäubler, Nat. Commun. **4**, 2291 (2013).
75. G. Lamporesi, S. Donadello, S. Serafini, F. Dalfovo, G. Ferrari, Nature Phys. **9**, 656 (2013).
76. W. H. Zurek, U. Dorner, Phil. Trans. R. Soc. A **366**, 2953 (2008).
77. B. Damski, W. H. Zurek, New J. Phys. **11**, 063014 (2009).
78. J. Dziarmaga and M. M. Rams, New J. Phys. **12**, 055007 (2010).
79. J. Dziarmaga and M. M. Rams, New J. Phys. **12**, 0103002 (2010).
80. M. Collura and D. Karevski, Phys. Rev. Lett. **104**, 200601 (2010).
81. J. E. Avron, R. Seiler, and L. G. Yaffe, Commun. Math. Phys. **110**, 33 (1987); **156**, 649 (1993).

82. H. Saberi, T. Opatrny, K. Mølmer, A. del Campo, arXiv:1408.0524 (2014).
83. S. Campbell, G. De Chiara, M. Paternostro, G. M. Palma, R. Fazio, arXiv:1410.1555 (2014).
84. A. Mostafazadeh, *Dynamical invariants, adiabatic approximation and the geometric phase*, (New York: Nova, 2001).
85. S. Ibáñez, Xi Chen, E. Torrontegui, J. G. Muga, and A. Ruschhaupt, Phys. Rev. Lett. **109**, 100403 (2012).
86. K. Takahashi, Phys. Rev. E **87**, 062117 (2013).
87. B. Damski, arXiv:1410.0059 (2014).
88. M. Müller, K. Hammerer, Y. L. Zhou, C. F. Roos, and P. Zoller, New J. Phys. **13**, 085007 (2011).
89. J. T. Barreiro, M. Müller, P. Schindler, D. Nigg, T. Monz, M. Chwalla, M. Hennrich, C. F. Roos, P. Zoller, and R. Blatt, Nature **470**, 486 (2011).
90. J. Casanova, A. Mezzacapo, L. Lamata, and E. Solano, Phys. Rev. Lett. **108**, 190502 (2012).
91. H. Weimer, M. Müller, I. Lesanovsky, P. Zoller, and H. P. Büchler, Nature Phys. **6**, 382 (2010).
92. V. F. Krotov, *Global Methods in Optimal Control Theory*, Dekker, New York, (1996); I. R. Sola, J. Santamaria, and D. J. Tannor, J. Phys. Chem. A **102**, 4301 (1998); S. A. Rice and M. Zhao, *Optical control of molecular dynamics* (Wiley, New York, 2000); N. Khaneja, T. Reiss, C. Kehlet, T. Schulte-Herbruggen, and S. G. Glaser, J. Magn. Res. **172**, 296 (2005); S. Montangero, T. Calarco, and R. Fazio, Phys. Rev. Lett. **99**, 170501 (2007); C. Brif, R. Chakrabarti, and H. Rabitz, New J. Phys. **12**, 075008 (2010); N. Eurich, M. Eckstein, and P. Werner, Phys. Rev. B **83**, 155122 (2011).
93. M. Mundt and D. J. Tannor, New J. Phys. **11**, 105038 (2009).
94. P. Doria, T. Calarco, and S. Montangero, Phys. Rev. Lett. **106**, 190501 (2011).
95. T. Caneva, T. Calarco, and S. Montangero, Phys. Rev. A **84**, 022326 (2011).
96. N. Wu, A. Nanduri, and H. Rabitz, arXiv:1409.1622 (2014).
97. M. A. Cazalilla, J. Phys. B: At. Mol. Opt. Phys. **37**, S1 (2004).
98. S. Lloyd, S. Montangero, arXiv:1407.6634 (2014).
99. L. Mandelstam and I. Tamm, J. Phys (USSR) **9**, 249 (1945).
100. G. N. Fleming, Nuov. Cim. **16 A**, 232 (1973).
101. K. Bhattacharyya, J. Phys. A **16**, 2993 (1983).
102. A. Uhlmann Phys. Lett. A **161**, 329 (1992).
103. N. Margolus and L. B. Levitin, Physica D **120**, 188 (1998).
104. S. Lloyd, Nature **406**, 1047 (2000); S. Lloyd, Phys. Rev. Lett. **88**, 237901 (2002); V. Giovannetti, S. Lloyd, and L. Maccone, Phys. Rev. A **67**, 052109 (2003).
105. P. Busch, Lect. Notes Phys. **734**, 73 (2008).
106. J. Anandan and Y. Aharonov, Phys. Rev. Lett. **65**, 1697 (1990).
107. P. Pfeifer, Phys. Rev. Lett. **70**, 3365 (1993).
108. X. Chen, J. G. Muga, Phys. Rev. A **82**, 053403 (2010).
109. S. Deffner, E. Lutz, J. Phys. A: Math. Theor. **46**, 335302 (2013).
110. M. M. Taddei, B. M. Escher, L. Davidovich, R. L. de Matos Filho, Phys. Rev. Lett. **110**, 050402 (2013).
111. A. del Campo, I. L. Egusquiza, M. B. Plenio, S. F. Huelga, Phys. Rev. Lett. **110**, 050403 (2013).
112. S. Deffner, E. Lutz, Phys. Rev. Lett. **111**, 010402 (2013).
113. A. Carlini, A. Hosoya, T. Koike, Y. Okudaira, Phys. Rev. Lett. **96**, 060503 (2006).
114. A. Carlini, A. Hosoya, T. Koike, Y. Okudaira, Phys. Rev. A **75**, 042308 (2007).
115. X. Wang, M. Allegra, K. Jacobs, S. Lloyd, C. Lupo, M. Mohseni, arXiv:1408.2465 (2014).
116. L.D. Landau, Phys. Z. Sowjetunion **2**, 46 (1932); G. Zener, Proc. R. Soc. London, Ser. A **137**, 696 (1932).
117. N. V. Vitanov and B. M. Garraway, Phys. Rev. A **53**, 4288 (1996).
118. In principle, one should evaluate  $c(t)$  at  $t = T$  instead of  $t = T_0$  as we have done; however, it is easy to see from the expression of  $T$  that this difference leads to subleading corrections which are irrelevant for the present purpose.
119. L. Jiang, T. Kitagawa, J. Alicea, A. R. Akhmerov, D. Pekker, G. Refael, J. I. Cirac, E. Demler, M. D. Lukin, P. Zoller, Phys. Rev. Lett. **106**, 220402 (2011).
120. We note that some recent experiments [see S.M. Griffin *et al.*, Phys. Rev. X **2**, 041022 (2012)] have reported suppression of defect density in multiferroic hexagonal manganites with increasing rate of temperature quench.
121. Y.-J. Lin, K. Jiménez-García, and I. B. Spielman, Nature (London) **471**, 83 (2011).
122. J. I. Cirac and P. Zoller, Nature Phys. **8**, 264 (2012).
123. M. Campisi, P. Hänggi, and P. Talkner, Rev. Mod. Phys. **83**, 771 (2011).
124. S. Boixo, G. Ortiz, R. Somma, arXiv:1409.2477 (2014).